Solitons in inharmonic lattices: Application to achiral carbon nanotubes

T. Yu. Astakhova*
Institute of Biochemical Physics, Russian Academy of Sciences, ul. Kosygina 4, Moscow 119991 GSP-1, Russia

Madhu Menon†
Department of Physics and Astronomy, University of Kentucky, Lexington, Kentucky 40506-0055, USA and Center for Computational Sciences, University of Kentucky, Lexington, Kentucky 40506-0045, USA

G. A. Vinogradov‡
Institute of Biochemical Physics, Russian Academy of Sciences, ul. Kosygina 4, Moscow 119991 GSP-1, Russia
(Received 17 October 2003; revised manuscript received 19 March 2004; published 15 September 2004)

In this paper we demonstrate that soliton solutions, whose existence is well known in one-dimensional (1D) model anharmonic systems, can also exist in more complex systems such as carbon nanotubes (CNT). We investigate armchair and zigzag nanotubes and show that both can be simplified to anharmonic 1D lattice models with reduced internal degrees of freedom. Because of the differences in chirality, the armchair and zigzag nanotubes are represented, respectively, by homogeneous (one site per unit cell) and dimerized chains. Starting with the Brenner potential we expand the tube energy into Taylor series and construct effective interaction potentials for model lattices of armchair and zigzag CNTs. We then construct a continuous approximation for the model lattices and derive the Korteweg–de Vries (KdV) equation by applying the reductive perturbation method. The stability of KdV solitons are checked by molecular dynamics simulations of model lattices with parameters specific for CNTs. Numerical simulations attest to the stability of even narrow solitons in most CNTs. We show that solitons can be generated by shock compression at one end of the model chains. The formalism developed can also be applied to many quasi-1D objects such as polymers, nanowires, and others.

DOI: 10.1103/PhysRevB.70.125409 PACS number(s): 65.40.Gr, 71.15.Pd, 71.20.Be, 75.40.Mg

I. INTRODUCTION

Carbon nanotubes (CNTs), discovered over a decade ago,[1] consist of graphene sheets rolled up into cylindrical shapes and possess a great aspect ratio. In many cases (e.g., electrical as well as heat conduction) their behavior closely resembles those of quasi-one-dimensional (Q1D) objects. Considerable efforts have been expended in elucidating the physical principles underlying the intriguing properties of CNTs,[2,3] and it has become clear that CNTs have many unique properties not shared by the bulk carbon materials.

One of these properties is heat conductance. Recent experiments have detected high values of thermal conductivity (κ) for both an individual CNT[4] and CNTs in suspension.[5] Calculations have also demonstrated a high value of κ,[6] but no firm theoretical background for high values of heat conduction has yet been laid out. Some authors have pointed to the unusually large phonon free path as a probable cause.[6] Alternatively, theoretical evidence suggests that model one-dimensional lattices describable with both harmonic and nonlinear potentials have anomalous heat conduction with no thermodynamical limit: $\kappa \propto N^{\alpha}$, where N is the number of particles in the chain, and $\alpha = 0.25 - 0.44$.[7] The validity of these conclusions in the case of Q1D objects such as CNTs is still questionable. The possibility also exists that the high values of κ may be caused by the presence of solitons. Solitons are known to be the eigenstates of some exactly solvable equations (Korteweg–de Vries, sine-Gordon, and a few others[8]) which are continuum approximations to some true 1D models, e.g., Fermi-Pasta-Ulam (FPU) chains[9] and Toda lattice.[10] Solitons as solitary excitations can travel large distances without suffering dissipation and can release their energy at defect sites in the lattice where favorable conditions for their propagation are absent. Solitons can be created by supplying some energy (using any mechanism) at one end of the chain, and once formed, they can propagate over large distances. It should be noted that there are several works where solitons are associated with CNTs. The first is devoted to dynamical solitons in a plane isotropic hexagonal lattice, treated using the Lennard-Jones interatomic potential.[11] Here the soliton represents a plane compression excitation moving along a certain crystallographic direction and having only one degree of freedom. Other works[12–14] deal with topological solitons in CNTs, analogous to those proposed for polyacetylenes.[15] In the present work we consider a different type of excitations in CNTs, dynamical excitations with three degrees of freedom resulting from the carbon–carbon nonlinear interactions. The present work aims to answer the question of whether solitons can exist in Q1D objects such as CNTs, and if they do how they can be generated experimentally.

In the present work we focus our efforts on obtaining solitonlike excitations in CNTs. In order to do this we treat CNTs as Q1D objects and reduce the problem to that of a 1D lattice with one, two, and three internal degrees of freedom per unit cell (denoted by 1DF, 2DF, and 3DF, respectively, to distinguish them from true one-, two-, and three-dimensional systems) and make use of parameters taken from the expansion of realistic classical potentials for CNTs. We then make continuum approximation for constructed models and derive

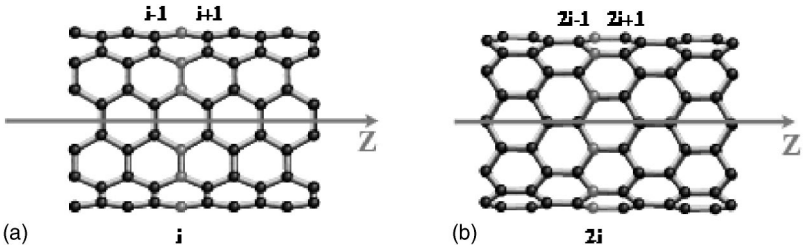

FIG. 1. (a) Armchair $(6,6)$ and (b) zigzag $(10,0)$ nanotubes.

the Korteweg–de Vries (KdV) equation by applying the reductive perturbation method.[16,17] In particular, we investigate two types of achiral CNTs: armchair and zigzag, which can be modeled by different lattices due to their different chiralities.

The paper is organized as follows: We begin by expanding Brenner's potential[18] in a series up to the third order, and in a symmetry-conserving assumption reduce the problem to a 3DF lattice with longitudinal, radial, and tangential degrees of freedom. In Sec. II we construct Q1D models for achiral CNTs and demonstrate that armchair and zigzag CNTs can be reduced to two different models; armchair CNTs to a homogeneous 3DF lattice, and zigzag CNTs to an inhomogeneous 2DF lattice. The two different model lattices for armchair and zigzag CNTs are considered separately. A homogeneous 3DF chain is considered in Sec. III, and an inhomogeneous 2DF chain is considered in Sec. IV. In both cases we first perform the analytical derivation of the KdV equation. This is then followed by a check of the stability of the derived soliton solution by numerical simulation of model lattices with CNT parameters corresponding to different diameters. Problems of soliton generation are discussed in Sec. V. Here we present the results of numerical simulations, where sets of solitons of different velocities and amplitudes are produced by a shock compression at one end of the model lattices for armchair and zigzag CNTs. The final section (Sec. VI) contains concluding remarks and discussions. There we also speculate on the possible role of solitons in different CNT processes.

II. LATTICE MODELS OF ACHIRAL CNTS

In this section we first demonstrate how model lattice systems can be used to represent achiral carbon nanotubes. In an earlier work[19] we had proposed a quasi-one-dimensional (Q1D) model for armchair CNTs. Here we briefly recall these results and construct a similar model for zigzag CNTs.

An armchair CNT (n,n) is shown in Fig. 1(a). We use cylindrical coordinates for convenience. We take the principal symmetry axis (nanotube axis) to be the Z axis, and allow longitudinal (ℓ), radial (ρ), and angular (φ) degrees of freedom. We take the (n,n) CNT to consist of a series of rings with each ring consisting of $2n$ atoms having the same Z coordinate.

Atoms belonging to the ith ring are shown with light circles in Fig. 1(a), and atoms in the neighboring $i-1$ and $i+1$ rings are shown with dark circles. The symmetry-preserving assumption involves assigning equal longitudinal (ℓ), radial (ρ), and tangential $(\sigma=R_{\text{tube}}\Delta\varphi)$ displacements from their equilibrium positions to all atoms in every ring subject to an excitation. This allows us to simplify the problem by reducing it to a lattice with three degrees of freedom per unit cell (3DF lattice), where each unit consists of $2n$ atoms in the ring. This assumption implies that all atoms of the ith ring have equal ℓ_i, ρ_i, and σ_i displacements, and no displacements of any other type inside the ring are permitted for the atoms in the ring. In other words, every ring whether moving along the nanotube axis or/and radially expanding or contracting does it as a whole. In Fig. 2(a) we illustrate the longitudinal, radial, and tangential displacements of atoms in two adjacent rings of armchair zigzag CNT. Here the left panel presents a portion of an armchair CNT consisting of two rings with atoms belonging to the first ring shown with light circles and atoms belonging to the next ring with dark circles. The central panel of Fig. 2(a) illustrates longitudinal displacements, the displacements of atoms in the first ring (dark circles) shown in thick short arrows, and displacements of atoms in the next ring (light circles) represented by long arrows. The atomic displacements under uniform expansion-contraction of every tube ring are shown in the right panel of Fig. 2(a). Because of nonsymmetric interaction in the plane perpendicular to the tube axis (in one direction every atom interacts with one atom within its own ring, and in another direction the atom interacts with two atoms of the adjacent two rings) the mode involves both radial and tangential displacements of every atom. Here, once again, both radial and tangential displacements of the atoms in the first ring (dark circles) are represented by thick short arrows, while the displacements of atoms in the next ring (light circles) are represented by long thin arrows. In other words, we wish to consider the simplest type of the dynamical mode, which can be generated, for example, by uniform compression of the

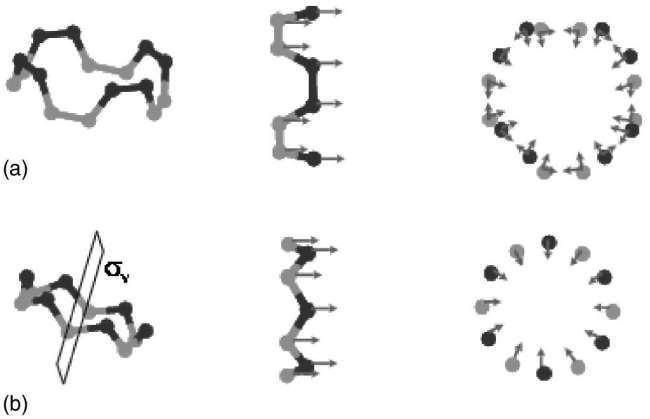

FIG. 2. Longitudinal, radial, and tangential displacements of atoms in two adjacent rings in armchair (a) and zigzag CNTs (b).

TABLE I. Numerical coefficients in the Taylor expansion of the Brenner potential for armchair CNTs (n,n).

Coefficient	(5,5)	(10,10)	(20,20)	(50,50)	(100,100)	(500,500)
c_1, eV/Å^2	30	30	30	30	30	30
c_2, eV/Å^3	75	75	75	75	75	75
c_3, eV/Å^2	1.4	0.7	0.4	0.1	0.04	0.001
c_4, eV/Å^2	4.8	1.2	0.3	0.03	0.01	0.01
c_5, eV/Å^2	20	20	20	20	20	20
c_6, eV/Å^2	125	125	125	125	125	125
c_7, eV/Å^2	12	6	3	1.2	0.5	0.2
Tube radius, Å	3.5	6.9	13.9	34.6	69.2	350.0

tube in the longitudinal direction, or by a uniform radial expansion.

Using the above assumptions one can start with a realistic potential for carbon such as the Brenner potential[18] and perform expansion in a series up to the third order term for the interaction energy between two nearest rings for an (n,n) armchair CNT of arbitrary n.[19] The expansion for the interaction energy between ith and $(i+1)$th rings is given by

$$E_{i,i+1} = \frac{1}{2}c_1(\ell_{i+1}-\ell_i)^2 - \frac{1}{3}c_2(\ell_{i+1}-\ell_i)^3 + c_3(\ell_{i+1}-\ell_i) \times(\rho_{i+1}+\rho_i) + \frac{1}{2}c_4\rho_i^2 + c_5(\ell_{i+1}-\ell_i)(\sigma_{i+1}+\sigma_i) + \frac{1}{2}c_6\sigma_i^2 - c_7\rho_i\sigma_i + O(\ell,\rho,\sigma), \quad (1)$$

where all nearest-neighbor interaction harmonic terms, one anharmonic term of the longitudinal variable [second term in Eq. (1)], and the cross terms are retained. The subscript i denotes the ring number, and $O(\ell,\rho,\sigma)$ denotes the discarded terms in the expansion. $O(\ell,\rho,\sigma)$ includes not only the higher-order terms of the third order and higher [except $(\ell_{i+1}-\ell_i)^3$], but also several second-order terms. That is the terms describing next-nearest-neighbor interaction are also omitted. These terms have the form $(x_{i+j}\pm x_i)^2$, where x is ℓ, ρ, or σ, and $j>1$. The second type of discarded second-order terms are those containing $(\rho_{i+1}-\rho_i)$ and/or $(\sigma_{i+1}-\sigma_i)$ expressions, since the expansion [Eq. (1)] includes second-order terms of $(\rho_{i+1}+\rho_i)$ and $(\sigma_{i+1}+\sigma_i)$ expressions and $(\rho_{i+1}-\rho_i)\ll(\rho_{i+1}+\rho_i)$ and $(\sigma_{i+1}-\sigma_i)\ll(\sigma_{i+1}+\sigma_i)$. Thus the expansion given by Eq. (1) now has a simple form which includes the longitudinal anharmonicity and allows the derivation of an analytical soliton solution. The validity of CNT description using the model potential in the form of Eq. (1) can be checked by numerical calculations only, where soliton evolution is modeled in real CNTs described through the Brenner potential. It would be a subject of future work and the aim of the present work is the derivation of analytical soliton and numerical examination of its stability in model lattices.

Note that the exact form of the initial potential is not essential in the construction of the model potential for CNTs; all potentials, empirical as well as those constructed from first principles, have the form of Eq. (1) with slightly different values of expansion coefficients, as this expansion is performed near the equilibrium.

The numerical values of coefficients in Eq. (1) are given in Table I for armchair CNTs of different diameters. Note that the expression given by Eq. (1) is the lowest-order expansion containing the minimum number of terms necessary for further derivations of desired solutions. As a result, the armchair CNT is represented by an anharmonic lattice described by the expansion in Eq. (1), where every unit has three internal degrees of freedom (ℓ, ρ, σ) and, therefore, can be considered as a 3DF homogeneous lattice.

We next turn our attention to zigzag $(n,0)$ CNTs. Once again, if the tube axis is aligned along the Z axis, then the tube can be thought of as consisting of a set of rings, with each ring formed by n atoms having the same Z value [see Fig. 1(b)]. Let us consider a two-ring portion of a zigzag CNT [see the left panel of Fig. 2(b)]. By taking the σ_v symmetry planes intersecting along the nanotube axis and passing through opposite atoms, it is easy to see that the uniform contraction/expansion of every tube ring does not contribute to the tangential displacement of atoms.

Thus the simplest dynamical mode in zigzag CNTs involve a displacement where all atoms belonging to the first ring have the same longitudinal [ℓ, see the central panel of Fig. 2(b)] and radial [r, see the right panel of Fig. 2(b)] displacements. Here again, the displacements of atoms marked by dark circles are shown by short thick arrows and the displacements of atoms marked by light circles are shown by long thin arrows.

Note that $(n,0)$ CNTs pose a severe challenge when attempting any analytical treatment as bonds connecting adjacent layers are not equivalent, and need to be divided into two subsets, denoted by "even" and "odd." Let the rings be numbered as shown in Fig. 1(b), i.e., rings formed by light circles are labeled even and rings formed by dark circles are labeled odd. It is easy to see that rings $2i$ and $2i+1$ are joined by n bonds, whereas the number of bonds between the $2i-1$th and $2i$th ring is $2n$. Thus the interaction of every ring with its two nearest neighbors is asymmetrical, and the zigzag nanotube should be considered as a dimerized lattice. We call this lattice an inhomogeneous one. As in the case of the armchair nanotube, the simplifying assumptions leading to

TABLE II. Numerical coefficients in the Taylor expansion of the Brenner potential for zigzag CNTs $(n,0)$.

Coefficient	(10,0)	(20,0)	(50,0)	(100,0)	(250,0)	(1000,0)
$\tilde{q}_1$, eV/Å^2	40	40	40	40	40	40
q_1, eV/Å^2	25	25	25	25	25	25
$\tilde{q}_2$, eV/Å^3	120	120	120	120	120	120
q_2, eV/Å^3	30	30	30	30	30	30
$\tilde{q}_3$, eV/Å^2	3.7	1.9	0.9	0.4	0.008	0
q_3, eV/Å^2	1.2	0.6	0.3	0.1	0.003	0
q_4, eV/Å^2	3.6	0.9	0.2	0	0	0
Tube radius, Å	4.0	8.0	20.0	40.0	100.0	400.0

the representation of a ring by a single lattice unit are still valid here.

Let us now consider a displacement mode where all atoms in one ring have the same longitudinal (ℓ) and radial (ρ) displacements without any tangential displacements. Then, the expansion of any realistic carbon potential for zigzag CNT will have the following form:

$$E_i = \frac{1}{2}\tilde{q}_1(\ell_i - \ell_{i-1})^2 + \frac{1}{2}q_1(\ell_{i+1} - \ell_i)^2 - \frac{1}{3}\tilde{q}_2(\ell_i - \ell_{i-1})^3 - \frac{1}{3}q_2(\ell_{i+1} - \ell_i)^3 + \tilde{q}_3(\ell_i - \ell_{i-1})(\rho_i + \rho_{i-1}) + q_3(\ell_{i+1} - \ell_i)(\rho_{i+1} + \rho_i) + \frac{1}{2}q_4\rho_i^2 + O(\ell,\rho), \quad (2)$$

where E_i is the interaction energy between the ith ring and its two neighboring rings, and expansion coefficients with and without the symbol "tilde" refer to inter-ring interaction through $2n$ and n bonds (odd-even and even-odd interactions), respectively, and $O(\ell,\rho)$ denotes all omitted terms as above. Again, only the essential terms are retained in the expansion in Eq. (2), and we use the assumption that zigzag CNTs can be modeled by a 2DF anharmonic inhomogeneous lattice interacting through the interatomic potential given by Eq. (2) with numerical values of coefficients given in Table II for zigzag tubes of different diameters. Note that equilibrium inter-ring distance in zigzag CNTs is essentially independent of the tube diameter and $\tilde{l}_o/l_o \approx 2$, where l_o and $\tilde{l}_o$ are equilibrium distances between rings $2i-1$, $2i$ and between rings $2i$, $2i-1$, respectively [see Fig. 1(b)].

In the next two sections we consider different models for armchair and zigzag CNTs in detail and derive the KdV equation for both models. The stability of KdV solitons are checked in numerical simulations.

III. MODELING ARMCHAIR CNTS

In this section we consider the 3DF model of armchair CNTs. First, we perform analytical treatment of the model lattice. Here we derive the KdV equation through construction of the continuum approximation of the model and apply the reductive perturbation method.[16,17] We then check the stability and the evolution of the derived solution by numerical simulations of the model lattice with numerical coefficients of the interaction potential [Eq. (1)] corresponding to armchair CNTs of different diameters (see Table I).

A. Analytical results

Let us consider a chain where every unit has three degrees of freedom ℓ, ρ, and σ and the interunit interaction potential is given by Eq. (1).

The equations of motion for the ith particle are

$$\begin{aligned}
\dot{\nu}_i &= c_1[(\ell_{i+1} - \ell_i) - (\ell_i - \ell_{i-1})] - c_2[(\ell_{i+1} - \ell_i)^2 - (\ell_i - \ell_{i-1})^2] \\
&\quad + c_3[(\rho_{i+1} + \rho_i) - (\rho_i + \rho_{i-1})] - c_5[(\sigma_{i+1} + \sigma_i) \\
&\quad - (\sigma_i + \sigma_{i-1})], \\
\dot{\mu}_i &= -c_3[(\ell_{i+1} - \ell_i) + (\ell_i - \ell_{i-1})] - c_4\rho_i + c_7\sigma_i, \\
\dot{v}_i &= c_5[(\ell_{i+1} - \ell_i) + (\ell_i - \ell_{i-1})] + c_7\rho_i - c_6\sigma_i, \\
\dot{\ell}_i &= \nu_i, \quad \dot{\rho}_i = \mu_i, \quad \dot{\sigma}_i = v_i. \qquad (3)
\end{aligned}$$

Hereafter, we set $m=1$ and take spatial variables in units of the equilibrium bond length $\ell_0=1$, making them dimensionless.

Next we construct a continuum approximation for the system [Eq. (3)] assuming small displacements from equilibrium positions and a long wavelength limit. Under these assumptions the displacements in Eq. (3) can be expanded in a series up to fourth order terms as follows:

$$\begin{aligned}
\ell_{i\pm1} &= \ell_i \pm \ell_i' + \frac{1}{2}\ell_i'' \pm \frac{1}{6}\ell_i''' + \frac{1}{24}\ell_i^{IV}, \\
\rho_{i\pm1} &= \rho_i \pm \rho_i' + \frac{1}{2}\rho_i'' \pm \frac{1}{6}\rho_i''' + \frac{1}{24}\rho_i^{IV}, \\
\sigma_{i\pm1} &= \sigma_i \pm \sigma_i' + \frac{1}{2}\sigma_i'' \pm \frac{1}{6}\sigma_i''' + \frac{1}{24}\sigma_i^{IV}. \qquad (4)
\end{aligned}$$

Spatial derivatives are denoted by primes hereafter. Substituting this expansion in Eq. (3) and introducing the new variable $\xi \equiv \ell'$, one gets the continuum approximation to the discrete system [Eq. (3)]:

$$\dot{\nu} = c_1\xi' + \frac{c_1}{12}\xi''' - c_2(\xi^2)' + 2c_3\rho' + \frac{c_3}{3}\rho''' - 2c_5\sigma' - \frac{c_5}{3}\sigma''',$$

$$\dot{\mu} = -2c_3\xi - \frac{c_3}{3}\xi'' - c_4\rho + c_7\sigma,$$

$$\dot{\upsilon} = 2c_5\xi + \frac{c_5}{3}\xi'' + c_7\rho - c_6\sigma,$$

$$\dot{\xi} = \nu', \quad \dot{\rho} = \mu, \quad \dot{\sigma} = \upsilon. \tag{5}$$

We next introduce a small number, ε, and expand all variables as

$$\xi = \varepsilon\xi_1 + \varepsilon^2\xi_2 \cdots,$$

$$\rho = \varepsilon\rho_1 + \varepsilon^2\rho_2 \cdots,$$

$$\sigma = \varepsilon\sigma_1 + \varepsilon^2\sigma_2 \cdots,$$

$$\nu = \varepsilon\nu_1 + \varepsilon^2\nu_2 \cdots,$$

$$\mu = \varepsilon\mu_1 + \varepsilon^2\mu_2 \cdots,$$

$$\upsilon = \varepsilon\upsilon_1 + \varepsilon^2\upsilon_2 \cdots. \tag{6}$$

Simultaneously, we transform the space and time coordinates as

$$\zeta \equiv \varepsilon^{1/2}(z - \upsilon_o t), \quad \tau \equiv \varepsilon^{3/2}t. \tag{7}$$

If we substitute Eqs. (6) and (7) into Eq. (5) and set terms of order $\varepsilon^{3/2}$ to be zero, then we get

$$\rho_1(\zeta,\tau) = a_1\xi_1(\zeta,\tau),$$

$$\sigma_1(\zeta,\tau) = a_2\xi_1(\zeta,\tau),$$

$$\nu_1(\zeta,\tau) = -\upsilon_o\xi_1(\zeta,\tau) + f(\tau),$$

$$\mu_1(\zeta,\tau) = a_1\dot{\xi}_1(\zeta,\tau),$$

$$\upsilon_1(\zeta,\tau) = a_2\dot{\xi}_1(\zeta,\tau), \tag{8}$$

where

$$\upsilon_o^2 = c_1 - 4\frac{c_3^2c_6 + c_4c_5^2 + 2c_3c_5c_7}{c_4c_6 - c_7^2},$$

$$a_1 = 2\frac{c_5c_7 - c_3c_6}{c_4c_6 - c_7^2},$$

$$a_2 = 2\frac{c_4c_5 - c_3c_7}{c_4c_6 - c_7^2}, \tag{9}$$

and f is an arbitrary function of τ. We put $f(\tau)=0$ since we seek a solution so that ξ, ρ, and σ tend to zero as $|\zeta| \to 0$.

Equating terms of order $\varepsilon^{5/2}$ to zero and taking into account Eqs. (8) and (9) we get the KdV equation for ξ_1

$$\dot{\xi}_1 - \alpha\xi_1\xi_1' + \beta\xi_1''' = 0, \tag{10}$$

where the dot and the prime mean partial derivatives with respect to new time τ and space ζ coordinates, and $\alpha=c_2$ and $\beta=\upsilon_o^2/12$.

One-soliton solution of the KdV equation [Eq. (10)] has the form

$$\xi_1 = A\ \mathrm{sech}^2 B(\zeta - \upsilon_{sol}\tau), \tag{11}$$

where

$$B^2 = \upsilon_{sol}/(4\beta), \quad A = -6\beta B^2/\alpha, \tag{12}$$

and other variables are expressed according to Eq. (8).

We next check numerically the soliton stability in a discrete parent 3DF chain with the potential given by Eq. (1) with coefficients c_1-c_7 appropriate for armchair CNTs. The soliton instability in the 3DF discrete chain may be attributed to two factors. The first is caused by the fact that the soliton is a solution of the continuum equation which, in turn, is an approximation to the discrete system under certain conditions. The second has to do with the fact that the soliton is only an approximate solution of the continuum equation.

B. Numerical simulations

Let us first consider the main features of the solution given by Eq. (11). Here, A is soliton amplitude and B is a parameter which is in inverse proportion to the soliton half-width w. One can easily check [see Eqs. (12) and (7)], that in the limit of infinite w the amplitude A tends to zero and soliton velocity approaches a certain value which is a sound velocity. If w tends to zero, on the other hand, both amplitude and the soliton velocity tend to infinity and we have a narrow width high-amplitude excitation traveling at high speed. Thus the lesser the soliton half-width w, the higher its velocity υ_{sol} as well as its amplitude, A.

One can also see that the smaller the tube diameter the slower the soliton. As will be shown below, it is a result of the presence of additional degrees of freedom (radial and tangential) interaction with main longitudinal degree of freedom and taking soliton energy. Numerical simulations show that the stronger the interaction between longitudinal, radial, and tangential degrees of freedom the lower the soliton stability.

One can see that the soliton amplitude is always negative ($A<0$), which implies that only solitons of compression exist, and no stable nonlinear elongation excitations of the type given by Eq. (11) can be obtained. This fact provides a useful tool in molecular dynamics (MD) simulations to check the existence of a real soliton in the lattice. If the excitation gets destroyed as a result of reversal of the sign of its amplitude, it is an evidence of a true soliton. This is an important test since harmonic excitations with small amplitudes and large half-widths are equally stable for both signs of relative atomic displacements. The differences in evolution of solitons with positive and negative amplitudes are due to the

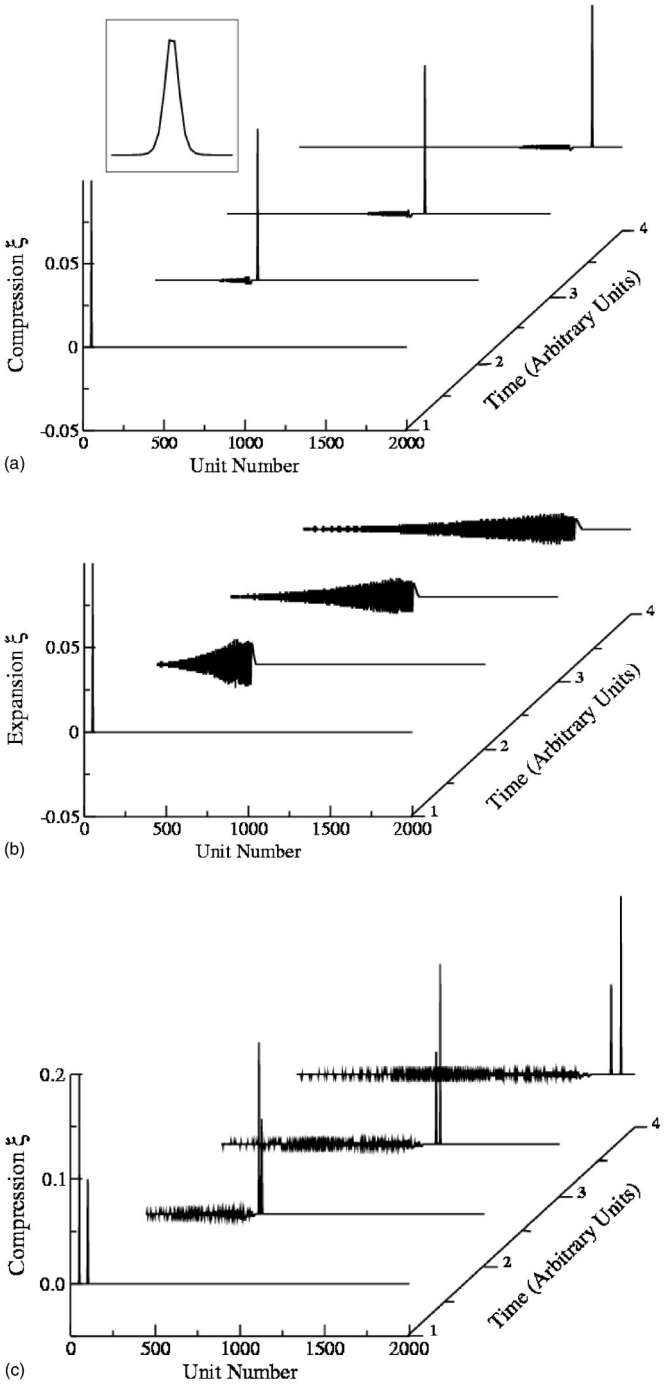

FIG. 3. MD simulations results for a 1DF homogeneous chain showing: (a) single soliton evolution, (b) evolution of the excitation after the reversal in the sign of amplitude and, (c) evolution of two solitons of different half-widths and velocities. Inset panel in (a) shows the front part of the fourth curve with a well-distinguished single soliton.

presence of the term $\alpha\xi_1\xi_1'$ in Eq. (10). In the case of a smaller excitation amplitude the second term in the left-hand side of Eq. (10) is much smaller than the first term and we have a wave equation describing the system where wide excitations with both signs of amplitude are highly stable.

The solution given by Eq. (11) is a supersonic soliton ($v_{sol} > v_{\text{sound}} = v_o$) with soliton half-width $w \approx 1.76/B$, where v_{sound} is the sound velocity in the model 3DF lattice. Parameters A, B, and v_{sol} are related by Eq. (12). That is, the choice of any one parameter is sufficient to determine others. Thus Eq. (11) describes a continuous set of one-parameter solitons. We find it convenient to choose w as a natural primary parameter.

We next present our results for numerical simulations of soliton evolution in model lattices. The numerical values of coefficients $c_1 - c_7$ are taken from the expansion in Eq. (1) (see Table I). We first consider 1DF chain modeling armchair CNTs with frozen radial and tangential modes. This case, in fact, is nothing other than the widely studied α-FPU problem.[9]

Generally, the wider the soliton, the greater its stability and consequently, one needs to investigate only the lower limit on soliton width required for stability. As a rule, the intrinsic characteristics of a soliton are vividly on display when the contribution of harmonic and nonlinear terms to the energy in Eq. (1) are comparable. This ensures that its amplitude is sufficiently large enough to be stable. It should be noted that solitons that are too narrow with a width comparable to the lattice spacing are considerably less stable.

We use two examples to demonstrate that solitons are stable in the 1DF discrete lattice. Our MD simulation results are shown in Fig. 3. Here we model a 1DF lattice with parameters $c_1 = 30$ and $c_2 = 75$ (see Table I). These coefficients do not depend on the tube diameter as they are determined by the local environment only.

The first example shows the case of a soliton undergoing a change in sign of its amplitude A in Eq. (11). The soliton is found to be very stable for $A < 0$ [Fig. 3(a)] and unstable for $A > 0$ [Fig. 3(b)]. A value $w \approx 2.5$ is chosen in both cases with $v_{sol} = 1.08 v_{\text{sound}}$ and $A \mp 0.1$, respectively. Small vibrations following the soliton are due to the discreteness of the lattice. These fluctuations become negligible as the soliton width gets larger. As can clearly be seen in Fig. 3(a), the soliton velocity exceeds the sound velocity represented by vibrational fluctuations.

Another essential soliton feature worth noting is the absence of any interaction on collision and it suffers only a phase shift.[8] Figure 3(c) illustrates the collision of two solitons when a narrower and faster soliton with larger amplitude runs over the slower one. Their half-widths are 1.8 and 2.5; amplitudes 0.2 and 0.1; and velocities $1.15 v_{\text{sound}}$ and $1.08 v_{\text{sound}}$, respectively.

Thus a simplified 1DF nonlinear discrete lattice containing parameters specific for CNTs can be a good model for solitons starting with a half-width as small as $w \geqslant 1$.

Let us now consider a 3DF lattice modeling an armchair CNT with all allowed degrees of freedom with variables ξ, ρ, and σ taken to be longitudinal, radial, and tangential degrees of freedom, respectively. For performing simulations of soliton evolution in the 3DF homogeneous lattice, we use parameters for armchair (n,n) nanotubes for $n = 10-100$ (see Table I). We find the soliton to be rather stable in almost all cases if its half-width is greater than $w = 0.8$. This is because of the high rigidity of the tangential mode which is the same for all tubes.

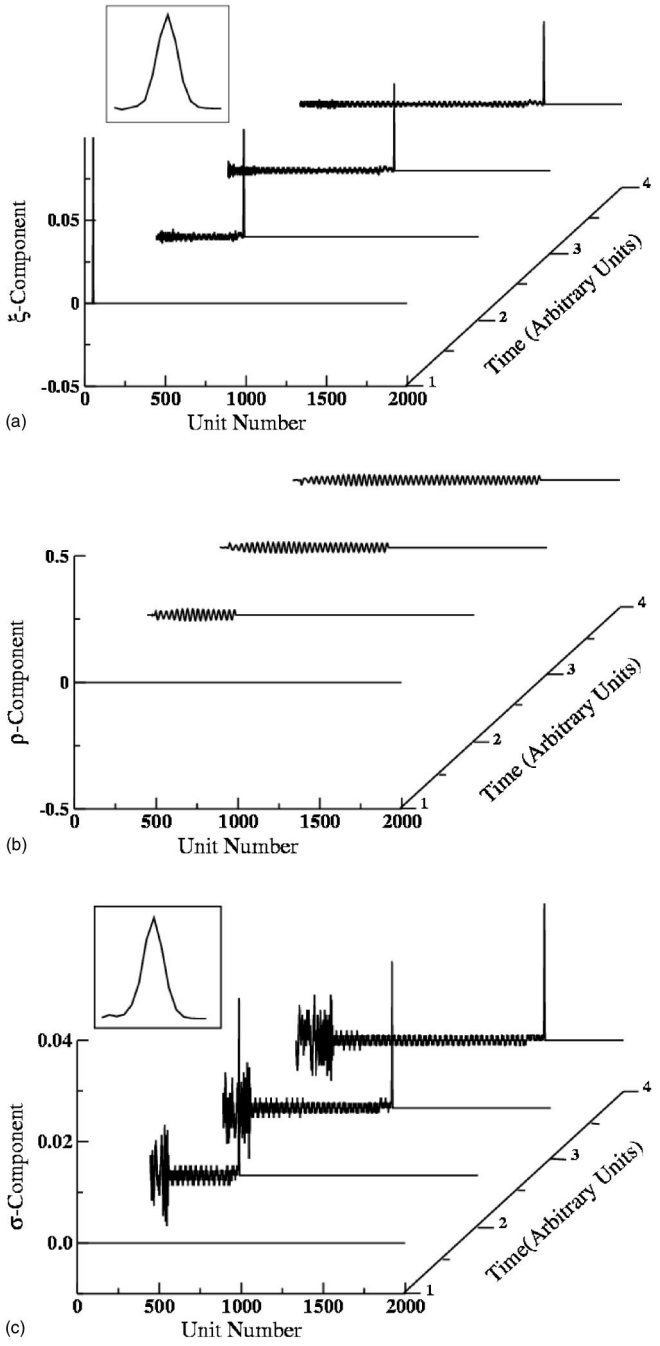

FIG. 4. Soliton evolution in 3DF homogeneous lattices with parameters for the (10,10) CNT: (a) ξ, (b) ρ, and (c) σ soliton components.

Figure 4 presents the soliton evolution in the 3DF lattices with parameters appropriate for a (10,10) tube (see Table I). Initial soliton parameters are taken to be $w=2.0$, $A=-0.1$, and $v_{sol}=1.12v_{\text{sound}}$. As seen in the figure, the soliton is very stable. The twofold behavior of the soliton can be seen here. While the ξ and σ components clearly reveal soliton features, radial component ρ shows regular features. This difference in the behavior can be attributed to the difference in the rigidity of the degrees of freedom; the longitudinal and tangential degrees of freedom are rigid and the radial degree of freedom is soft (see Table I). The numerical simulations show that for the whole range of parameters corresponding to armchair CNTs of different diameters, the radial degree of freedom behaves as a soft mode, i.e., only oscillations of the ρ mode are observed. So, it serves as an energy reservoir, slowly absorbing the soliton energy and transforming it to the vibrations at a rate depending on the strength of interaction between all degrees of freedom.

We next turn our attention to zigzag CNTs which can be modeled by a different lattice; i.e., by an inhomogeneous 2D anharmonic lattice (see Sec. II).

IV. LATTICE MODELS OF ZIGZAG CNTS

Let us consider the expansion in Eq. (2) for zigzag CNTs, which is really an inhomogeneous nonlinear lattice with two internal degrees of freedom, longitudinal and radial. Simulations using the Brenner potential show that there is no contribution to the tangential degree of freedom when an excitation is created in which all atoms of one ring have equal radial and longitudinal displacements. We, therefore, exclude the tangential degree of freedom from any further consideration. Unlike the (n,n) CNTs, model lattices for the zigzag CNTs are dimerized lattices with two particles per unit cell, where particle masses are equal, but the force constants differ.

A. Analytical results

Let us consider the inhomogeneous 2DF chain with two internal degrees of freedom ℓ and ρ and the interaction energy described by Eq. (2). Because of the two types of bonds in the chain we consider equations of motion for the even ℓ_{2i}, ρ_{2i} and odd ℓ_{2i-1}, ρ_{2i-1} coordinates, separately. The equations of motion are

$$\ddot{\ell}_{2i} = q_1(\ell_{2i+1} - \ell_{2i}) - \tilde{q}_1(\ell_{2i} - \ell_{2i-1}) - q_2(\ell_{2i+1} - \ell_{2i})^2 + \tilde{q}_2(\ell_{2i} - \ell_{2i-1})^2 + q_3(\rho_{2i+1} + \rho_{2i}) - \tilde{q}_3(\rho_{2i} + \rho_{2i-1}),$$

$$\ddot{\ell}_{2i-1} = \tilde{q}_1(\ell_{2i} - \ell_{2i-1}) - q_1(\ell_{2i-1} - \ell_{2i-2}) - \tilde{q}_2(\ell_{2i} - \ell_{2i-1})^2 + q_2(\ell_{2i-1} - \ell_{2i-2})^2 + \tilde{q}_3(\rho_{2i} + \rho_{2i-1}) - q_3(\rho_{2i-1} + \rho_{2i-2}),$$

$$\ddot{\rho}_{2i} = -q_3(\ell_{2i+1} - \ell_{2i}) - \tilde{q}_3(\ell_{2i} - \ell_{2i-1}) - q_4\rho_{2i},$$

$$\ddot{\rho}_{2i-1} = -\tilde{q}_3(\ell_{2i} - \ell_{2i-1}) - q_3(\ell_{2i-1} - \ell_{2i-2}) - q_4\rho_{2i-1}. \tag{13}$$

We then introduce new variables $\eta_i=\ell_{2i}$, $\tilde{\eta}_i=\ell_{2i-1}$, $\varrho_i=\rho_{2i}$, $\tilde{\varrho}_i=\rho_{2i-1}$, $\nu_i=\dot{\ell}_{2i}$, $\tilde{\nu}_i=\dot{\ell}_{2i-1}$, $\mu_i=\dot{\rho}_{2i}$, and $\tilde{\mu}_i=\dot{\rho}_{2i-1}$, and as in the previous case, we make a continuum approximation assuming small displacements from the equilibrium positions and long wavelength limit. Under these assumptions the deviations in new variables are expanded as

$$\eta_{i\pm1} = \eta_i \pm \eta_i' + \frac{1}{2}\eta_i'' \pm \frac{1}{6}\eta_i''' + \frac{1}{24}\eta_{IV}^i,$$

$$\tilde{\eta}_{i\pm1} = \tilde{\eta}_i \pm \tilde{\eta}_i' + \frac{1}{2}\tilde{\eta}_i'' \pm \frac{1}{6}\tilde{\eta}_i''' + \frac{1}{24}\tilde{\eta}_i^{IV},$$

$$\varrho_{i\pm1} = \varrho_i \pm \varrho_i' + \frac{1}{2}\varrho_i'' \pm \frac{1}{6}\varrho_i''' + \frac{1}{24}\varrho_i^{IV},$$

$$\tilde{\varrho}_{i\pm1} = \tilde{\varrho}_i \pm \varrho_i' + \frac{1}{2}\tilde{\varrho}_i'' \pm \frac{1}{6}\tilde{\varrho}_i''' + \frac{1}{24}\tilde{\varrho}_i^{IV}. \tag{14}$$

Substituting this expansion in Eq. (13) and introducing two new variables $\xi \equiv \eta'$ and $\tilde{\xi} \equiv \tilde{\eta}'$, one gets the continuum approximation to the discrete system [Eq. (13)]:

$$\begin{aligned}\dot{\nu} &= (q_1\xi - \tilde{q}_1\tilde{\xi}) + \frac{1}{2}(q_1\xi' + \tilde{q}_1\tilde{\xi}') + \frac{1}{6}(q_1\xi'' - \tilde{q}_1\tilde{\xi}'') \\ &+ \frac{1}{24}(q_1\xi''' + \tilde{q}_1\tilde{\xi}''') - (q_2\xi^2 - \tilde{q}_2\tilde{\xi}^2) - \frac{1}{4}[q_2(\xi')^2 + \tilde{q}_2(\tilde{\xi}')^2] \\ &- (q_2\xi\xi' - \tilde{q}_2\tilde{\xi}\tilde{\xi}') + 2(q_3\varrho - \tilde{q}_3\tilde{\varrho}) + (q_3\varrho' + \tilde{q}_3\tilde{\varrho}') \\ &+ \frac{1}{2}(q_3\varrho'' - \tilde{q}_3\tilde{\varrho}'') + \frac{1}{6}(q_3\varrho''' + \tilde{q}_3\tilde{\varrho}'''),\end{aligned}$$

$$\begin{aligned}\dot{\tilde{\nu}} &= (\tilde{q}_1\tilde{\xi} - q_1\xi) + \frac{1}{2}(\tilde{q}_1\tilde{\xi}' + q_1\xi') + \frac{1}{6}(\tilde{q}_1\tilde{\xi}'' - q_1\xi'') \\ &+ \frac{1}{24}(\tilde{q}_1\tilde{\xi}''' + q_1\xi''') - (q_2\xi^2 - \tilde{q}_2\tilde{\xi}^2) - \frac{1}{4}[q_2(\xi')^2 + \tilde{q}_2(\tilde{\xi}')^2] \\ &- (q_2\xi\xi' - \tilde{q}_2\tilde{\xi}\tilde{\xi}') + 2(q_3\varrho - \tilde{q}_3\tilde{\varrho}) + (q_3\varrho' + \tilde{q}_3\tilde{\varrho}') \\ &+ \frac{1}{2}(q_3\varrho'' - \tilde{q}_3\tilde{\varrho}'') + \frac{1}{6}(q_3\varrho''' + \tilde{q}_3\tilde{\varrho}'''),\end{aligned}$$

$$\dot{\mu} = -(q_3\xi + \tilde{q}_3\tilde{\xi}) - \frac{1}{2}(q_3\xi' - \tilde{q}_3\tilde{\xi}') - \frac{1}{6}(q_3\xi'' + \tilde{q}_3\tilde{\xi}'') - q_4\varrho,$$

$$\dot{\tilde{\mu}} = -(\tilde{q}_3\tilde{\xi} + q_3\xi) - \frac{1}{2}(\tilde{q}_3\tilde{\xi}' - q_3\xi') - \frac{1}{6}(\tilde{q}_3\tilde{\xi}'' + q_3\xi'') - q_4\tilde{\varrho},$$

$$\dot{\tilde{\xi}} = \tilde{\nu}', \quad \dot{\xi} = \nu',$$

$$\dot{\rho} = \mu,$$

$$\dot{\tilde{\rho}} = \tilde{\mu}. \tag{15}$$

Then, as in the previous case, we introduce a small number ε and expand all variables as

$$\begin{aligned}q_1\xi &= \varepsilon u_1 + \varepsilon^2 u_2 + \cdots, \\ \tilde{q}_1\tilde{\xi} &= \varepsilon u_1 - \varepsilon^2 u_2 + \cdots, \\ \varrho &= \varepsilon\varrho_1 + \varepsilon^2\varrho_2 + \cdots, \\ \tilde{\varrho} &= \varepsilon\varrho_1 + \varepsilon^2\varrho_2 + \cdots, \\ q_1\nu &= \varepsilon v_1 + \varepsilon^2 v_2 + \cdots, \\ \tilde{q}_1\tilde{\nu} &= \varepsilon v_1 - \varepsilon^2 v_2 + \cdots, \\ \mu &= \varepsilon\mu_1 + \varepsilon^2\mu_2 + \cdots, \\ \tilde{\mu} &= \varepsilon\mu_1 + \varepsilon^2\mu_2 + \cdots.\end{aligned} \tag{16}$$

Simultaneously, we suppose that

$$\begin{aligned}(q_1\tilde{q}_2 - \tilde{q}_1 q_2)/ &\approx \varepsilon^2(q_1\tilde{q}_2 + \tilde{q}_1 q_2), \\ q_3\tilde{q}_3/q_4 &\approx \varepsilon^2\sqrt{q_1\tilde{q}_1},\end{aligned} \tag{17}$$

which indicates the presence of weak anharmonicity in the system and also the weak interaction between ξ and ρ degrees of freedom.

Thus, transforming the space and time coordinates as in the previous case [Eq. (7)], taking into account Eqs. (16) and (17), and equating terms of order $\varepsilon^{3/2}$ to be zero we get

$$\begin{aligned}\varrho_1(\zeta,\tau) &= a u_1(\zeta,\tau), \\ v_1(\zeta,\tau) &= -v_o u_1(\zeta,\tau) + f(\tau),\end{aligned} \tag{18}$$

where

$$\begin{aligned}v_o^2 &= \frac{2q_1\tilde{q}_1}{q_1 + \tilde{q}_1} - \frac{(q_3 + \tilde{q}_3)^2(\tilde{q}_1 q_3 + q_1\tilde{q}_3)^2}{(q_1 + \tilde{q}_1)^2 q_4}, \\ a &= \frac{\tilde{q}_1 q_3 + q_1\tilde{q}_3}{q_1\tilde{q}_1 q_4},\end{aligned} \tag{19}$$

and f is an arbitrary function of τ. We put $f(\tau)=0$ since we find such a solution that ξ and ρ tend to zero as $|\zeta| \to 0$.

Equating terms of order $\varepsilon^{5/2}$ to zero and taking into account Eqs. (18) and (19) we get the KdV equation for u_1

$$\dot{u}_1 - \alpha u_1 u_1' + \beta u_1''' = 0, \tag{20}$$

where the dot and the prime mean partial derivatives with respect to new time τ and space ζ coordinates, correspondingly, and $\alpha = (q_1^2\tilde{q}_2 + \tilde{q}_1^2 q_2)/q_1(q_1 + \tilde{q}_1)\tilde{q}_1$ and $\beta = v_o^2/12$. The one-soliton solution of Eq. (20) is then given by Eq. (11).

B. Numerical simulations

We next investigate the soliton evolution in 2DF inhomogeneous lattices by numerical methods. We have verified the soliton stability in 2DF inhomogeneous lattices with parameters appropriate for zigzag CNTs of different diameters. We

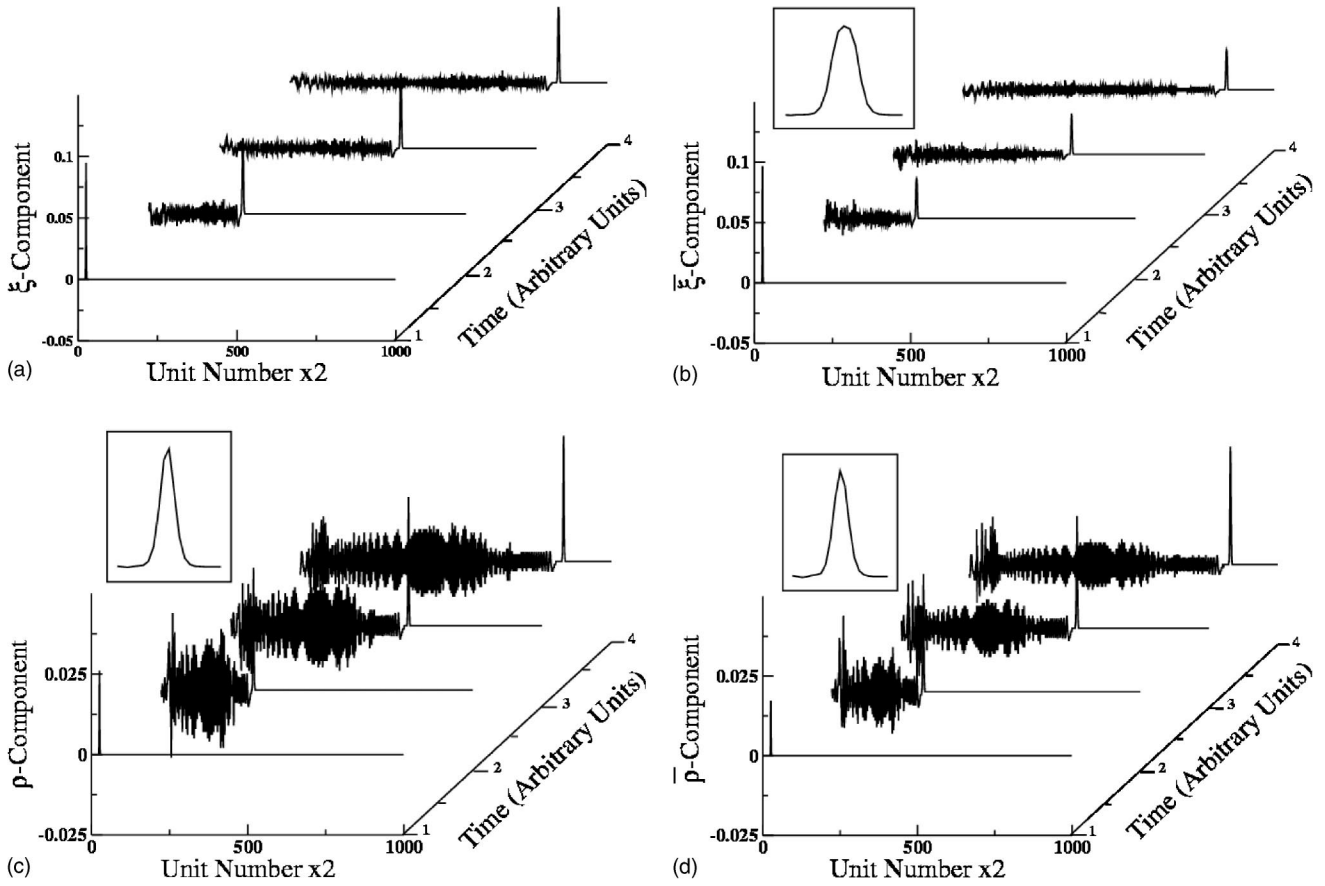

FIG. 5. Soliton evolution in 2DF inhomogeneous lattice with parameters for a $(10,0)$ CNT: (a) $\tilde{\xi}$, (b) ξ, (c) $\tilde{\varrho}$, and (d) ϱ components of soliton variables. The total number of units in the lattice modeled is 2000. So the number of variables $\tilde{\xi}$ and ξ is 1000. This explains the multiplication factor of 2 in the caption for the x axis.

tested coefficients q_1-q_4 and $\tilde{q}_1-\tilde{q}_4$ in Eq. (2) corresponding to zigzag $(n,0)$ tubes for $n=10-200$ (see Table II) and find that solitons are stable in all cases. An example is shown in Fig. 5 for parameters q_1-q_4, $\tilde{q}_1-\tilde{q}_4$ corresponding to the $(10,0)$ tube. Here we present evolutionary pictures for all $\tilde{\xi}$, ξ, $\tilde{\varrho}$, and ϱ components. Initial soliton parameters are $w=3.1$, $v_{sol}=1.1v_{\text{sound}}$. One can see that soliton features are well distinguished for all components, and the ratio of $\tilde{\xi}$ and ξ amplitudes is very close to the value $q_1/\tilde{q}_1$, which confirms the assumption that in the first appriximation $q_1\xi\approx\tilde{q}_1\tilde{\xi}$ in Eq. (16). The vibrations left behind by the solitons are due to the discreteness of the lattice and approximations made in Eqs. (16) and (17). One can, thus, conclude that solitons do exist and are rather stable in 2DF inhomogeneous lattices which are models for zigzag CNTs.

V. SOLITON GENERATION BY SHOCK COMPRESSION

The numerical simulations presented in this work have demonstrated high soliton stability. In all numerical calculations solitons survive for a long time moving along the chain consisting of thousands of atoms. We next turn our attention to the physical reasons responsible for giving rise to soliton generation under normal conditions. It should be noted that the initial conditions used in our calculations were of a special type [see Eq. (11)] requiring highly coordinated displacements and velocities of particles. It is difficult, if not impossible, to imagine external natural sources capable of producing such highly coherent excitations. The question arises, therefore, if solitons can exist in real systems describable by the KdV equation, and in particular, in CNTs. Or, in other words, whether naturally occurring initial conditions can produce solitons. If the answer is "yes" then what is the precise form of these initial conditions?

The answer to this question is contained in the spectral theory (see, for example, Ref. 8). It predicts that in a system described by the KdV equation a wide range of initial conditions result in a series of solitons of different velocities and amplitudes, and solitons are separated with time evolution due to the differences in their velocities. The initial conditions resulting in soliton generation should include a narrow and strong compression of one end of the chain; and initial shock compression is one of the ways to produce such initial conditions.

Following these ideas we next simulate soliton generation by shock compression. A shock compression has a rectangular profile and can be formed by the application of an external force at one end of the chain. The value of the applied force in the simulations is three units[23] and its duration 250 MD steps (each MD step $\approx$0.35 fs). We investigated

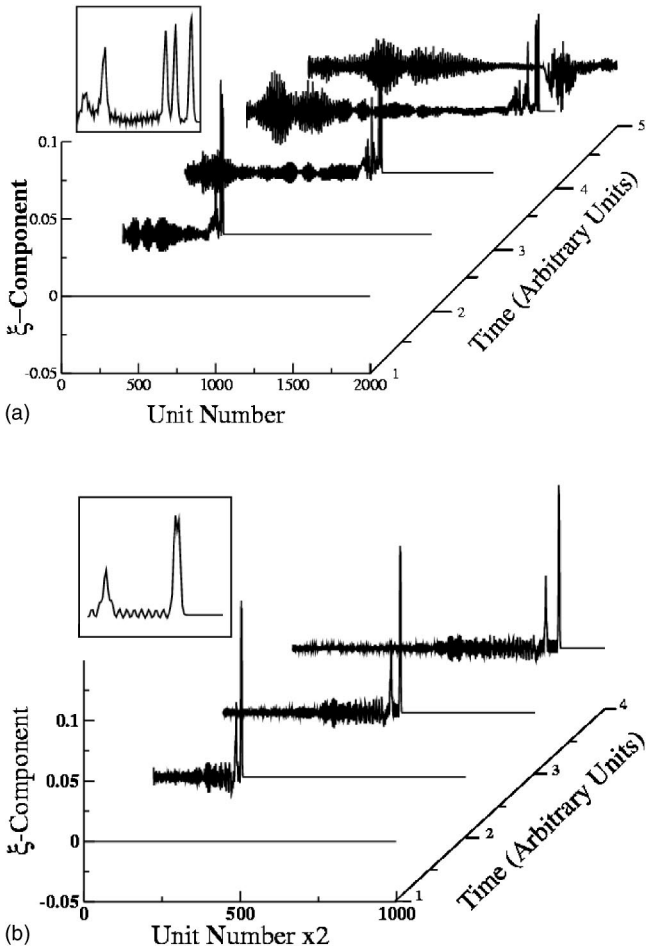

FIG. 6. Soliton generation by initial shock compression applied to the left end of the chain: (a) ξ component of 3DF chain and (b) ξ component of 2DF homogeneous chain. Inset panels show front part of fourth curve with distinguished set of solitons of the corresponding picture.

both model lattices for armchair and zigzag CNTs. The results are presented in Fig. 6. In both cases the external action is the same.

In Fig. 6(a) we present the results for a 3DF homogeneous chain. Here we only give the evolution of the ξ component, sufficient for observing the solitons generation. Similarly, in the case of a 2DF inhomogeneous chain we also present the evolution of only the ξ component as shown in Fig. 6(b).

As seen in Fig. 6, the initial impulse, after traveling some distance, splits into a set of well separated solitons with different amplitudes with the larger the amplitude, the greater its speed. As a result solitons are aligned according to their amplitudes. The soliton with the largest amplitude has the largest velocity and the least half-width (right most soliton) as predicted by the theory [Eq. (12)]. To verify the soliton nature of the solitary waves formed, we allow them to reflect from the free end of the chain [see fifth curve in Fig. 6(a)]. The reflection causes the set of compression excitations to transform into elongation excitations which are not eigenstates of the lattice and, therefore, easily destroyed. Note that fixed boundary conditions, on the other hand, preserve the compression nature of the excitations, and solitons survive after reflection in this case. Oscillations are dissipated due to the discreteness of the chain.

By observing similarities in the evolution of ξ variables in Figs. 4(a) and 6(a) it is easy to see that Fig. 6(a) can be obtained by a superposition of evolution pictures of solitons of different half-widths. Note that a close-up view of the propagating soliton [inset in Fig. 4(a)] shows that we have clearly identified a single solitary excitation. This means that an initially formed excitation is close to being an eigenstate of the system, confirming the validity of the analytical approximation made in Sec. IIIA. Numerical analysis shows that the number of solitons generated depends on the amplitude and duration of the shock compression. It is quite possible to choose initial conditions in such a way as to obtain a single soliton.

Theory and numerical simulations thus show that solitons are easily produced by initial shock compression applied at one end of the chain. Therefore solitons should be observed when similar external action is applied to the systems which can be modeled by any anharmonic chain.

VI. CONCLUSIONS

Since it is not possible to obtain an exact soliton solution for real CNTs, we avoided using the contemporary mathematical theory of solitons (see, e.g., Refs. 20 and 21) and instead focused on developing a semiquantitative approach assuming the existence of approximate solutions having the form of KdV solitons. Particular attention was paid to verifying the stability of obtained solutions using molecular dynamics simulations.

Our results can be summarized as follows: Armchair and zigzag nanotubes have different chiralities and, hence, can be modeled by distinct lattices; armchair by homogeneous 3DF lattice and zigzag can be modeled by inhomogeneous 2DF lattice. Our results show that soliton solutions can indeed exist in both models with parameters appropriate for real CNTs. The presence of solitons in these systems is caused by the nonlinear longitudinal interaction between nanotube rings. The required leading terms in the expansion of any potential necessary for simulating solitons are harmonic and cubic terms of the longitudinal variable.

The radial and tangential degrees of freedom seem to have a negative effect on the solitons. Radial and tangential degrees of freedoms are found to absorb some soliton energy, turning it into thermal or irregular vibrations. The more rigid the radial-tangential mode, the less the interaction between longitudinal and radial-tangential modes and the more stable the soliton. The soliton stability depends on the relations between the parameters corresponding to longitudinal, radial, and tangential modes. Obviously, the larger the diameter of the modeled nanotube, the more stable is the soliton.

Nevertheless, numerical calculations show that solitons are stable even in tubes of small diameters, i.e., solitons travel through thousands of rings without suffering any significant changes in form and amplitude. Thus numerical calculations prove that the method applied is suitable for the derivation of approximate solutions. We have also shown that solitons can be easily generated by initial shock com-

pression applied at one end of the chain. This leads to the expectation that solitons can be observed experimentally when similar external action is applied to the systems which can be modeled by any anharmonic chain.

Our method and results obtained from it can be useful in the treatment of solitary excitations in other Q1D systems such as nanowires, linear polymers, and other similar structures. Currently very little is known about the possible role of solitons in different physical processes in Q1D systems, in part because of a lack of reliable experimental results. We can, however, point to a few possibilities. For example, soliton-assisted electron drag can be expected to be more pronounced than a phonon-assisted phenomenon.[22] The close relation between electronic structure and geometry in CNTs opens up the possibility of electromechanical effects and piezoelectricity. The role of solitons in heat conductance in Q1D systems, including CNTs, is still unresolved and further investigations are needed.

In the present work we were interested mainly in the nonlinear dynamical properties of achiral carbon nanotubes and neglected the electronic properties. The reason being that the geometric perturbations caused by the solitons are usually too small to induce any significant changes in the electronic structure. We do, however, plan to include the investigation of the soliton-electron interaction in the future even though we expect the soliton contribution to the electronic structure to be negligible. The situation is very different in the case of inelastic interaction of solitons with defects (cap, free ends, etc.) in the nanotubes. These effects were described in our previous paper where effects on the electronic structure were considered.[19]

ACKNOWLEDGMENTS

This work was supported by research grants from Russian Foundation for Basic Research (02-02-16205, 04-03-32119, and 04-02-17306), Presidium of RAS "Fundamental Problems of Physics and Chemistry of Nanosized Systems and Nanomaterials," Presidium of RAS "Low-Dimensional Quantum Structures." M.M. gratefully acknowledges support from NSF Grant No. ITR-0221916, DOE Grant No. 00-63857, NASA Grant No. 00-463937, and the Kentucky Science & Technology Corporation (KSTC-0360214).

*Electronic address: astakhova@deom.chph.ras.ru
†Electronic address: super250@pop.uky.edu
‡Electronic address: gvin@deom.chph.ras.ru

[1] S. Iijima, Nature (London) **354**, 56 (1991).
[2] R. Saito, G. Dresselhaus, and M. S. Dresselhaus, *Physical Properties of Carbon Nanotubes* (Imperial College Press, London, 1998).
[3] M. Dresselhaus, G. Dresselhaus, and P. Avouris, *Carbon Nanotubes: Topics in Applied Physics* (Springer-Verlag, Berlin, 2001).
[4] P. Kim, L. Shi, A. Majumdar, and P. L. McEuen, Phys. Rev. Lett. **87**, 215502 (2001).
[5] S. U. S. Chou, Z. G. Zhang, W. Yu, F. E. Lockwood, and E. A. Grulke, Appl. Phys. Lett. **79**, 2252 (2001).
[6] S. Berber, Y. K. Kwon, and D. Tomanek, Phys. Rev. Lett. **84**, 4613 (2000).
[7] S. Lepri, R. Levi, and A. Politi, Phys. Rep. **377**, 1 (2003).
[8] F. Calogero and A. Degasperis, *Spectral Transform and Solitons: Tools to Solve and Investigate Nonlinear Evolution Equations* (North-Holland Amsterdam, 1982), p. 1.
[9] E. Fermi, J. Pasta, and S. Ulam, Los Alamos Report No. LA-1940, 1955.
[10] M. Toda, *Theory of Non-linear Lattices* (Springer, Berlin, 1981).
[11] Y. Zolotaryuk, A. V. Savin, and P. L. Christiansen, Phys. Rev. B **57**, 14213 (1998).
[12] C. Chamon, Phys. Rev. B **62**, 2806 (2000).
[13] M. T. Figge, M. Mostovoy, and J. Knoester, Phys. Rev. Lett. **86**, 4572 (2001).
[14] M. T. Figge, M. Mostovoy, and J. Knoester, Phys. Rev. B **65**, 125416 (2002).
[15] A. J. Heeger, S. Kivelson, J. R. Schriffer, and W. P. Su, Rev. Mod. Phys. **60**, 781 (1988).
[16] T. Taniuti and C. C. Wei, J. Phys. Soc. Jpn. **24**, 941 (1968).
[17] K. Sasaki, Prog. Theor. Phys. **65**, 1787 (1981).
[18] D. W. Brenner, Phys. Rev. B **42**, 9458 (1990).
[19] T. Y. Astakhova, O. D. Gurin, M. Menon, and G. A. Vinogradov, Phys. Rev. B **64**, 035418 (2001).
[20] A. C. Newell, *Solitons in Mathematics and Physics* (Society for Industrial and Applied Mathematics, Philadelphia, 1985).
[21] G. L. J. Lamb, *Elements of Soliton Theory* (Wiley, New York, 1980).
[22] V. W. Scarola and G. D. Mahan, Phys. Rev. B **66**, 205405 (2002).
[23] The force value is in units of the Brenner potential (Ref. 18) where energy is given in eV, length in Å, and the mass of carbon atom is taken to be 1.